Chapter 5

Structural Effect on α-Synuclein Caused by Two Single-point Mutations Related to Familial Parkinson's Disease

5.1 ABSTRACT

Two single-point mutations in the α-synuclein sequence (A30P and A53T) have been linked to familial Parkinson's disease. These mutations are compelling evidence that α-synuclein is involved in the pathogenesis of this neurodegenerative disorder. Fluorescent energy transfer is yet again utilized to provide time-resolved fluorescent decays of eight of the previously studied tryptophan-3-nitrotyrosine donor-acceptor pairs. Distance distributions can be extrapolated from these decays to investigate whether these single point mutations can lead to any structural change in solution and various membrane mimics. The effect on the calcium binding ability of the C-terminal tail was also explored.

5.2 INTRODUCTION

Two missense mutations in the α-syn sequence, namely A30P[1] and A53T[2], have been linked to early onset Parkinson's disease. One of the roles of these two mutations is to accelerate the formation of protofibrils, which has been considered as the toxic species causing PD.[3] The rate of fibril formation between wild type, A30P, and A53T α-syn has been investigated.[4-8] Although it has been demonstrated that all three α-syn sequences are capable of producing fibrils that are similar to the ones extracted from Lewy bodies, the rate of fibril formation is the fastest for the A30P mutant, while A53T mutant is the slowest.[9] However, both mutations have demonstrated capability of generating protofibrils faster than wild type α-syn.[9-11] These evidence suggests that although both A30P and A53T could lead to PD, their pathogenesis pathways should be different.

AFM studies suggested that A53T α-syn can disrupt membranes more than wild type α-syn,[12] while other studies have shown that A30P α-syn has a weaker binding affinity toward lipid membranes.[12-15] Another AFM study showed that protofibrils are in the form of spheres, with A30P forming tighter spheres than wild type. On the other hand, A53T protofibrils contain a mixture of spheres, with the tight spheres resembling those commonly found in A30P.[16] These AFM studies showed that there should be differences in structures between wild type, A30P, and A53T α-syn. Therefore, it is in our interest to compare the structure of monomeric α-syn with these single point mutations to further understand the disease.

Previous studies completed by NMR and EPR have stated that the N-terminal region of α-syn demonstrates a highly helical structure in the presence of SDS micelles or acidic SUVs.[17-22] This region is also marked by characteristic seven eleven-residue repeats.[23] Since this region is highly structured in the presence of membrane mimics, the presence of these alanine mutations can possibly disrupt these structures. In Chapter 3, we have obtained the distance distributions for N-terminal mutants in solution, SDS micelles, and 1:1 POPC:POPA SUV using fluorescent energy transfer (FET).

In this study, we are interested in studying whether the introduction of these point mutations leads to any changes in the structure of monomeric α-syn. Previously studied D-A pairs were incorporated into A30P or A53T and fluorescent energy transfer (FET) was employed, where tryptophan has been utilized as the fluorescent donor, and 3-nitrotyrosine has been selected as the energy acceptor. Previously, Lee et al. has utilized similar techniques, using W4/Y19(NO_2)/A30P and Y19(NO_2)/W39/A30P, to conclude that the introduction of A30P can cause more relaxed structures to be formed in the N-terminal helix.[24] In this study, the effectsof A53T mutant on this helix were investigated using W4/Y19(NO_2)/A53T and Y19(NO_2)/W39/A53T. Furthermore, Y39(NO_2)/W94 and Y74(NO_2)/W94 were selected to the effect of both missense mutations on the C-terminal helix. W39/Y55(NO_2) was elected to study the linker region of α-syn.

In Chapter 4, the calcium binding ability of the α-syn C-terminal tail has been demonstrated. Therefore, three of the C-terminal mutants studied, namely W94/Y113(NO_2), W94/Y125(NO_2), and W125/Y136(NO_2), were also chosen to

compare the structural changes caused by the alanine point mutations in solution and SUVs. The effect of calcium ions on these mutants was also investigated.

5.3 METHODS

Protein expression, purification, nitration, and characterization have been outlined in Chapter 1. The data collection parameters for steady-state and time-resolved fluorescence measurements have also been previously described. However, it is important to note that spectroscopic studies on the N-terminal mutants were carried out in 20 mM NaP_i (pH 7.4), while 10 mM HEPES buffer (pH 7.4) was used for C-terminal mutants. SDS micelles and 1:1 POPC:POPA SUVs were made in the appropriate buffers, determined by the mutants to be studied.

5.4 RESULTS AND DISCUSSIONS

N-terminal Helix.

In **Figure 5.1a**, we can observe that the distance distributions extracted from W4/Y19(NO_2) (blue) and W4/Y19(NO_2)/A53T (green). A slightly tighter conformation was formed in W4/Y19(NO_2)/A53T when it was associated with membrane mimics. It can be extrapolated that a slightly tighter helix was formed when these mutants were in association with micelles than with SUVs. This trend is opposite from what A30P can affect the N-terminal helix.

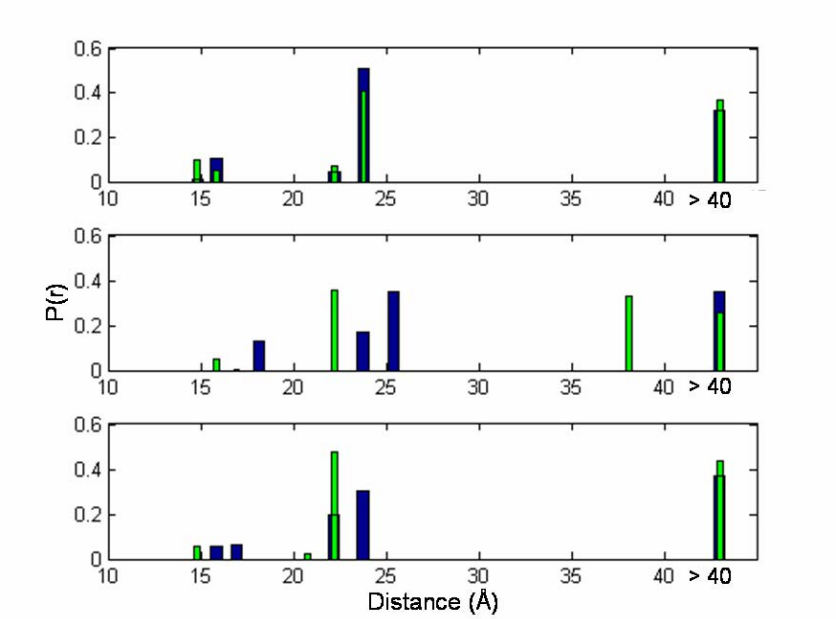

(a)

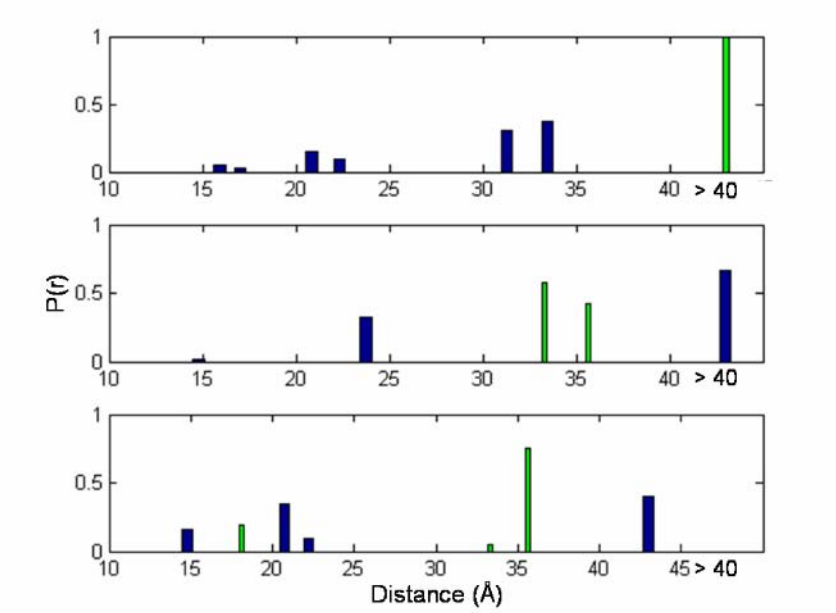

(b)

Figure 5.1. D-A distance distributions extrapolated from FET kinetics for **(a)** W4/Y19(NO_2) (blue) and W4/Y19(NO_2)/A30P (red), **(b)** Y19(NO_2)/W39 and Y19(NO_2)/W39/A53T (green) in 20 mM NaP_i buffer (top panel), 1:1 POPC:POPA (middle panel), and 31 mM SDS (bottom panel)

On the contrary, although Y19(NO_2)/W39 and W4/Y19(NO_2) are located within the same N-terminal helix, the effects caused by A53T are noticeably different (**Figure 5.1b**). When Y19(NO_2)/W39/A53T was placed in solution, only extended distances (> 40 Å) are found. When it was in association with SUVs, a shorter distance (~ 34 Å, 100%) in SUVs is formed. But, when the mutant was bound to the smaller membrane mimic, SDS micelles, a population (20%) of short distance (18 Å) emerges. Previously, we have shown that the N-terminal helix formed similar structures in micelles and SUVs. However, the distance distributions displayed by this A53T mutat in micelles show a much larger scale of contraction. This implies that A53T can possibly prevent this portion of the N-terminal helix from forming close contact in solution. However, in the presence of small membrane mimics, a much tighter helix can be formed.

Lee et al. has previously studied the effect of A30P on this mutant also.[24] They have concluded that the presence of that mutant allows a higher distribution of extended distances when the mutant was in association with micelles. Our results demonstrate that an opposite phenomenon is observed when A53T is incorporated into these N-terminal mutants. Therefore, we can conclude that A30P and A53T mutations affect the structure of monomeric α-syn quite differently.

C-terminal Helix.

In Chapter 3, we have postulated that C-terminal helix forms a tighter helix with the α-syn mutant is associated with SDS micelles than with SUVs. In **Figure 5.2**, the distance distributions for Y74(NO_2)/W94 (blue), Y74(NO_2)/W94/A30P (red), and Y74(NO_2)/W94/A53T (green) are shown. Y74(NO_2)/W94/A30P in solution is the only one that shows some intermediate distances (~ 23 Å, ~ 60%) and short distances (~ 15 Å, ~ 10%). All the other intermediate and short distance distributions in Y74(NO_2)/W94 in various environments have disappeared.

Although it is known that A30P and A53T mutants both form helices in these regions, it is possible that this C-terminal helix is now in a more relaxed conformation. This phenomenon is also supported by the data presented in **Figure 5.3**, where the only non-extended distances could only be observed when Y39(NO_2)/W94/A30P was placed in buffer. These results also suggest that the presence of the A30P and A53T mutations can prevent this polypeptide region from forming close contacts.

Linker Region.

W39/Y55(NO_2) is studied to investigate the behavior of the linker region and also the C-terminal helix. From **Figure 5.4b**, it shows that the A53T mutant provides longer distance distributions in solution when compared to the pseudo wild-type mutant. This implies that A53T could weaken any propensity for the unstructured protein from forming close contacts.

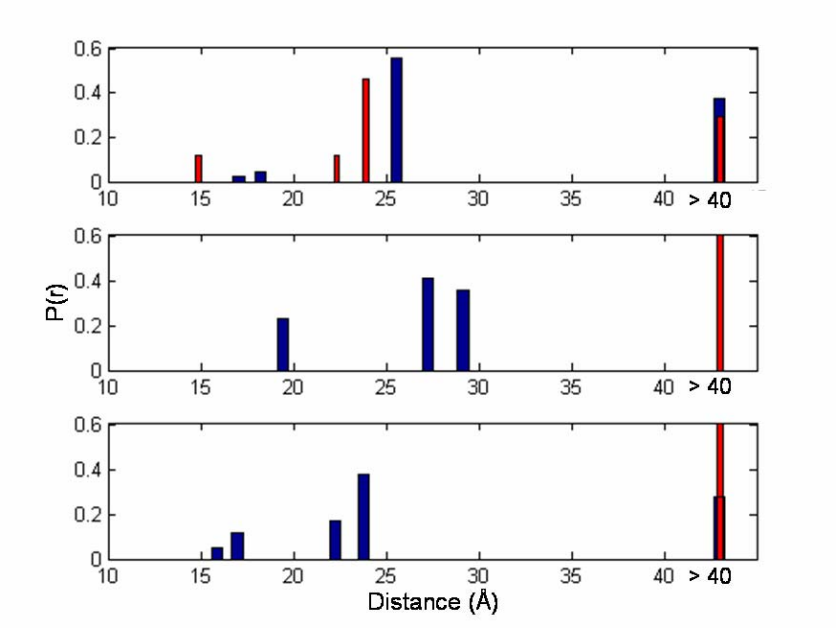

(a)

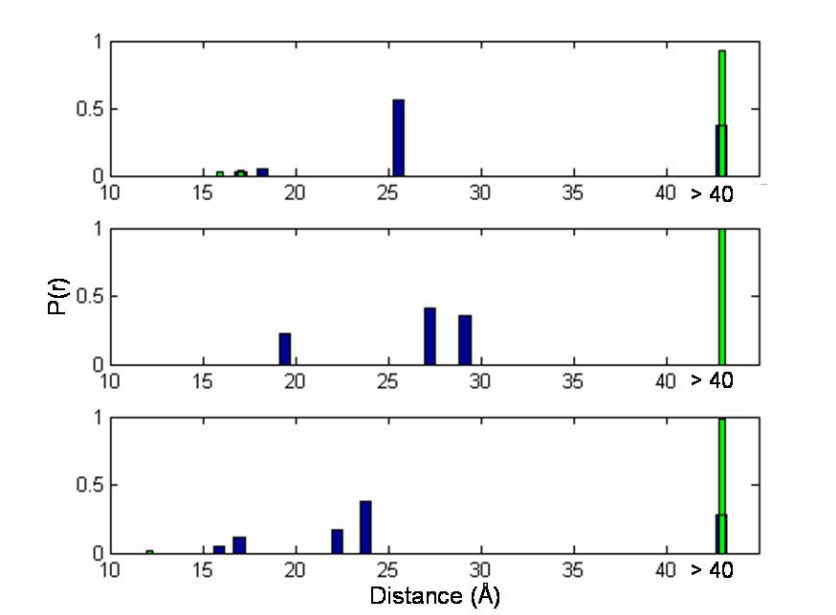

(b)

Figure 5.2. D-A distance distributions extrapolated from FET kinetics for Y74(NO_2)/W94 (blue), **(a)** Y74(NO_2)/W94/A30P (red), and **(b)** Y74(NO_2)/W94/A53T (green) in 20 mM NaP_i buffer (top panel), 1:1 POPC:POPA (middle panel), and 31 mM SDS (bottom panel)

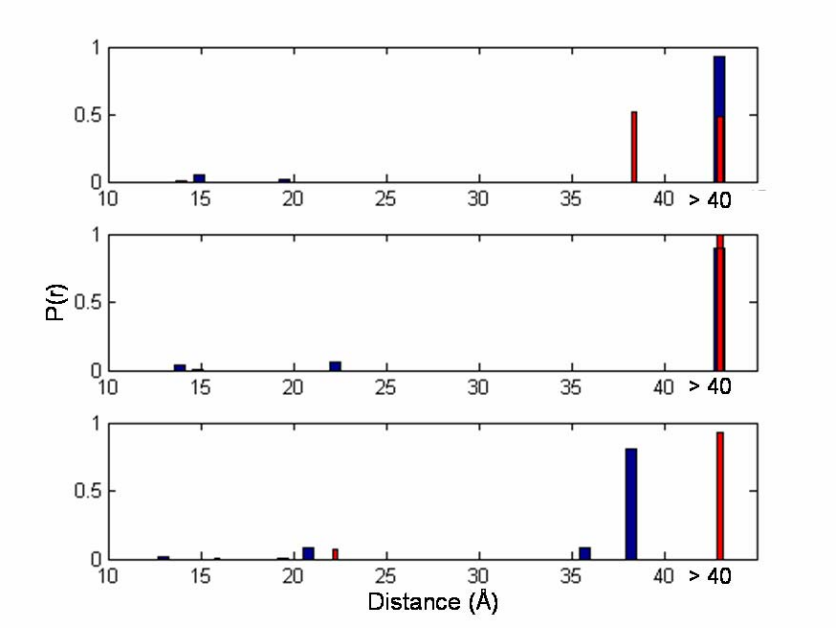

(a)

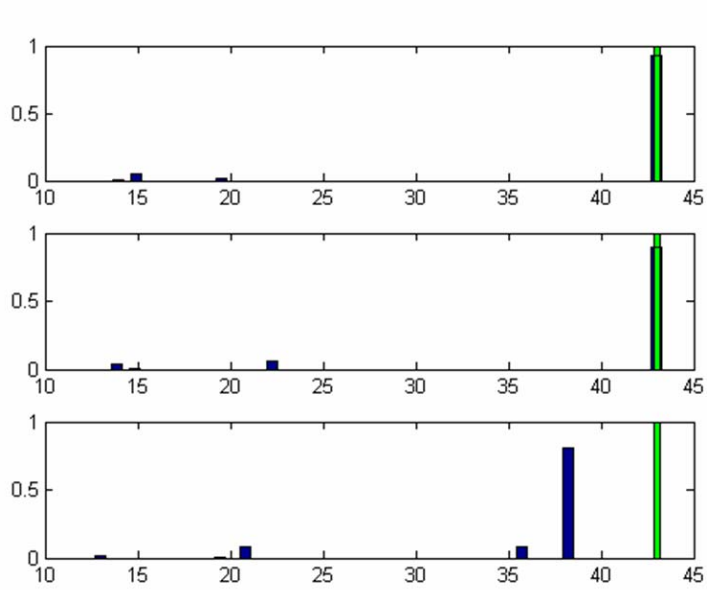

(b)

Figure 5.3. D-A distance distributions extrapolated from FET kinetics for Y39(NO_2)/W94 (blue), **(a)** Y39(NO_2)/W94/A30P (red), and **(b)** Y39(NO_2)/W94/A53T (green) in 20 mM NaP_i buffer (top panel), 1:1 POPC:POPA (middle panel), and 31 mM SDS (bottom panel)

On the other hand, the extended distance population (> 40 Å) has increased from ~ 40% to ~ 60% in membrane mimics. Conversely, the intermediate distance populations (~ 20 Å) have shifted to smaller distances. The presence of the A53T mutant can shorten the turn region, thus justifying the shortening of the intermediate distance populations. On the other hand, the lengthening of the extended distance population can further confirm that the C-terminal helix becomes more relaxed when the A53T mutation is introduced.

In the pseudo wild-type mutant, the distance distribution shows that a tighter helix is formed in the presence of SDS micelles when compared to SUVs. This similar trend is still observed for the A53T mutant, only the distance reduction is at a smaller extent. This also implies that the C-terminal helix of the A53T mutant could still be folding into similar motif like its pseudo wild type counterpart, only with a looser helix and tighter turn area. On the other hand, for W39/Y55(NO_2)/A30P (**Figure 5.4a**), an opposite trend can be observed, where a more compact distance distribution is found when the mutant is bound to SUVs than to micelles.

It is also interesting to note that in solution, the A30P mutant gives a shorter distance for the compact distances region (~ 20 Å) when compared to the non-disease mutant, possibly implying the effect of A30P in the turn region (**Figure 5.4a**). On the contrary, the extended distances distribution (> 33 Å) becomes more extended when the A30P mutant is introduced. Previously, we have shown that the introduction of the A30P can discourage close contacts from forming for the C-terminal mutants (Y74/Y94(NO_2) and Y39/W94(NO_2)), thus causing this lengthening phenomenon.

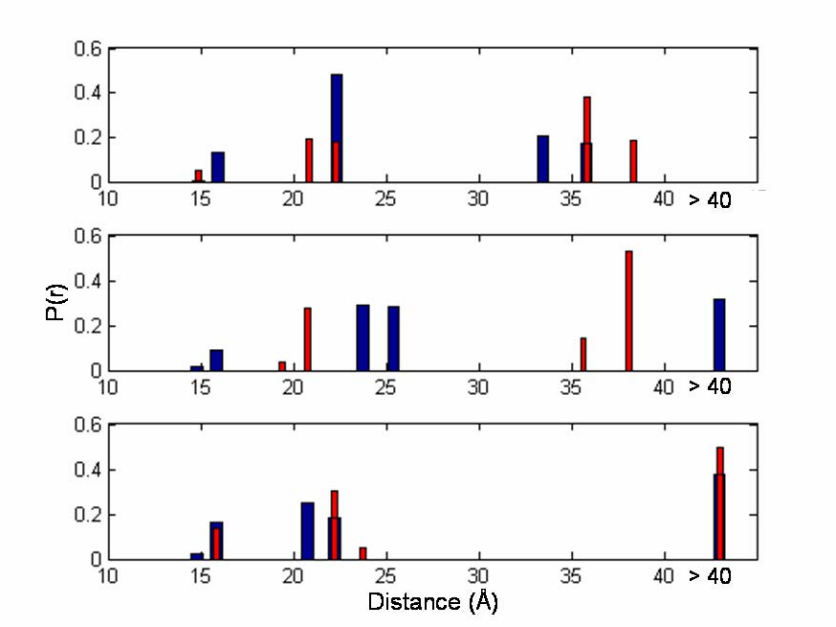

(a)

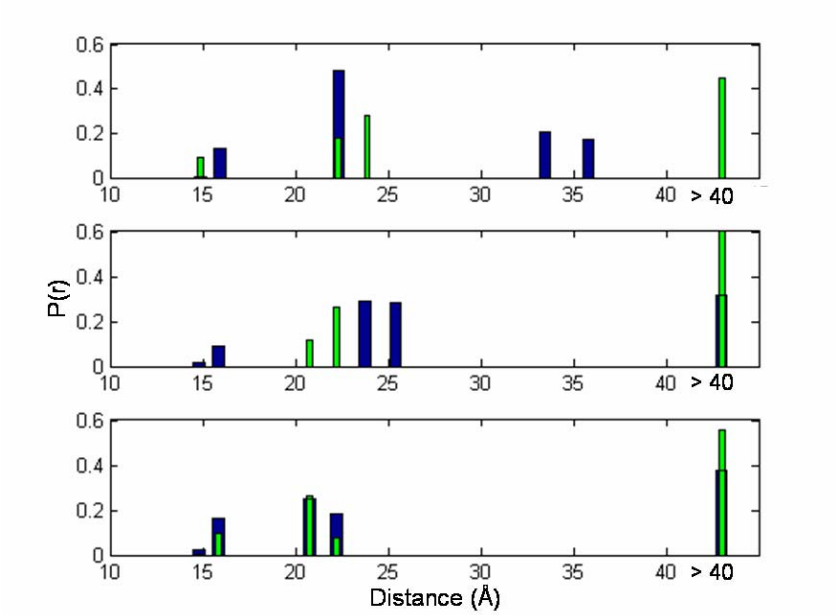

(b)

Figure 5.4. D-A distance distributions extrapolated from FET kinetics for W39/Y55(NO_2) (blue), **(a)** W39/Y55(NO_2)/A30P (red), and **(b)** W39/Y55(NO_2)/A53T (green) in 20 mM NaP_i buffer (top panel), 1:1 POPC:POPA (middle panel), and 31 mM SDS (bottom panel)

Summary on the helical region.

Figure 5.5a shows a summary on the effect of A30P (red arrows) and A53T (green arrows) mutations on the structure in solution, when compared to their non-disease related counterpart. It shows that both mutations discourage the formation of close contacts in the second half of the N-terminal mutant. On the other hand, A30P allows the C-terminal helix to form close contact easier, while preventing it in the turn region and the second part of the N-terminal helix. However, opposing phenomenon can be observed for the A53T mutant.

Figure 5.5b and **Figure 5.5c** show that the effect of A30P and A53T are quite similar when the mutants are in association with SUVs and micelles. They both cause the C-terminal helix to lengthen and the turn region to contract. The only difference is that it does not seem that the A30P can cause shortening of distances in the second half of the N-terminal helix in SUVs, while A53T has that effect on that region for both membrane mimics. From these results, it can suggest that the contraction in the second half of the N-terminal helix could be a culprit for the seeding the aggregation reaction. Since the NAC region (residues 61–95) is suspected of being involved in the pathogenesis of the PD, the lengthening of the C-terminal helix could also affect aggregation.

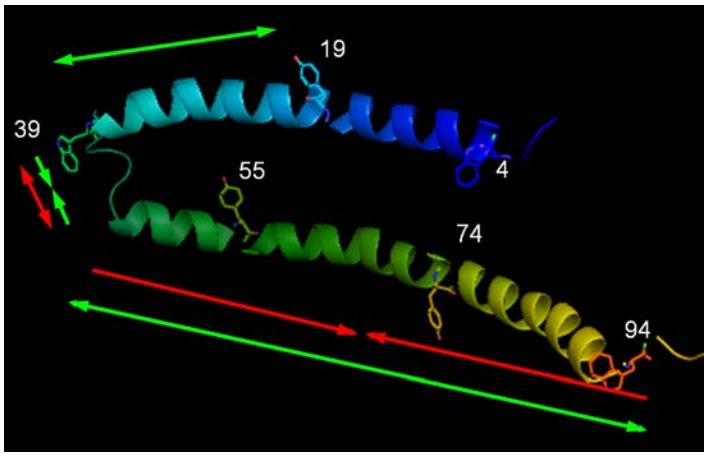

(a)

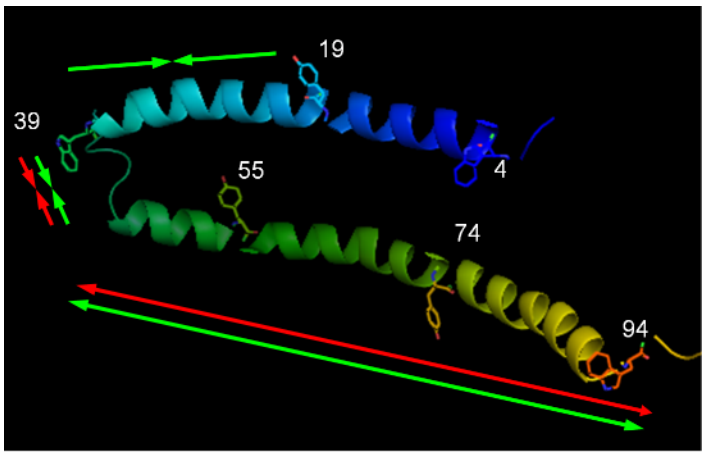

(b)

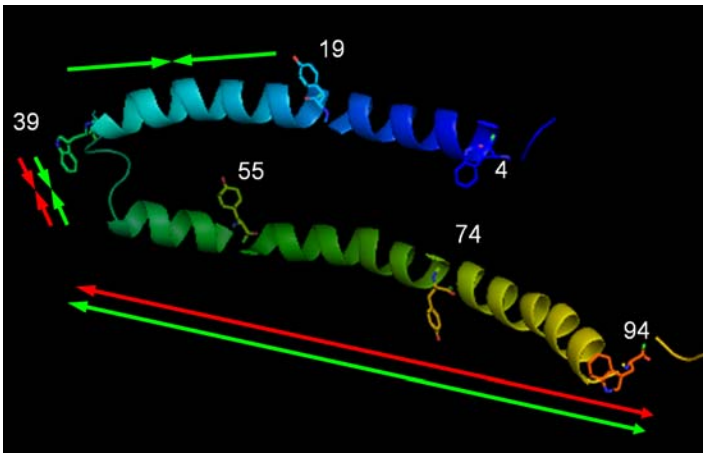

(c)

Figure 5.5. The effect of A30P (red) and A53T (green) mutants on the structure of α-syn in **(a)** NaPi, **(b)** SUVs, and **(c)** SDS micelles, when compared with their pseudo-wild-type counterpart

C-terminal Tail in Solution.

For the mutant W125/Y136(NO_2), more compact structures formed when the A30P and A53T mutations were introduced (**Figure 5.6**). There is also a small contraction of distance distributions (60%) from 22 Å to 21 Å for the A30P mutant when calcium ions were added. Similar shortening of distances (23 Å to 21 Å, 60%) can be observed in W125/Y136(NO_2)/A53T. However, these decreases in distances are smaller in scale compared to the mutants without these single-point mutations. Previously in Chapter 4, we have elucidated a calcium binding pocket between residues 125 and 136 in solution; it seems like this binding motif is maintained with the introduction of A30P or A53T, with the possibility that they weaken the calcium binding ability.

Figure 5.7 shows the addition of A30P and A53T into the W94/Y113(NO_2) mutation causes an increase in the population of extended distances (> 40 Å), with A30P showing a more dramatic change (60%) compared to A53T (10%). In addition, a more dramatic shift of the short distance distribution is observed for A30P than A53T. These general trends can be observed regardless of whether calcium ions are present, implying that A30P and A53T can lead to more compact structures.

It is also interesting to note although there is no change in the population of the extended distances when calcium ions are introduced, there is a contraction observed on the short distance population, with the A30P mutant shifting ~ 3 Å, while the A53T mutant only yields a ~ 1 Å change. We have previously assigned a calcium binding region between residues 101 and 113 in solution. From this set of data, it suggests that this calcium binding region remains with the A30P/A53T mutations.

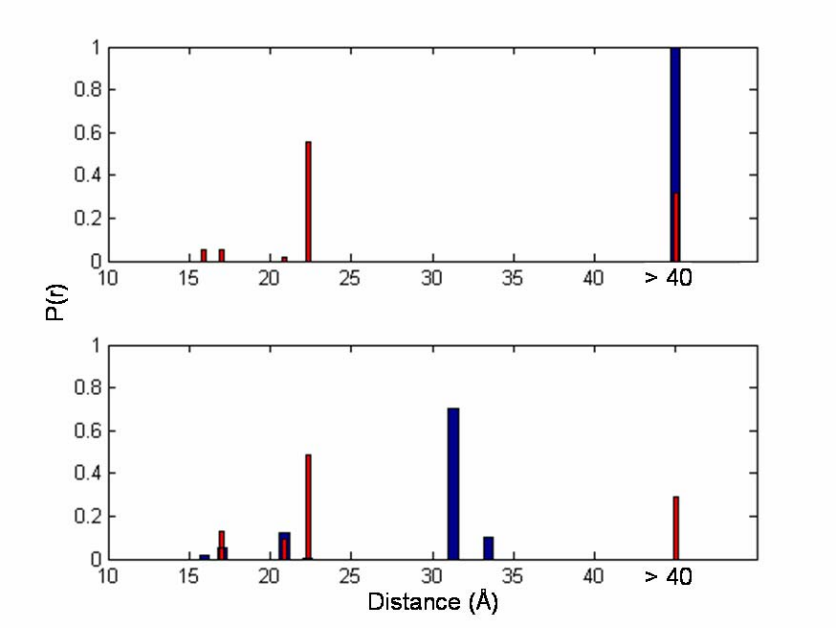

(a)

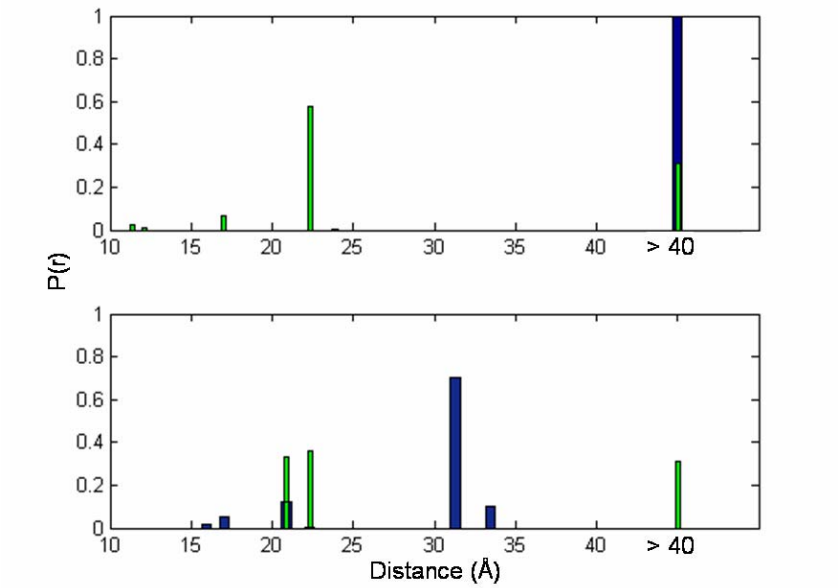

(b)

Figure 5.6. D-A distance distributions extrapolated from FET kinetics for W125/Y136(NO_2) (blue), **(a)** W125/Y136(NO_2)/A30P (red), and **(b)** W125/Y136(NO_2)/A53T (green) in 10 mM HEPES buffer (top panel), and 10 mM HEPES buffer with 1 mM Ca^{2+} (bottom panel)

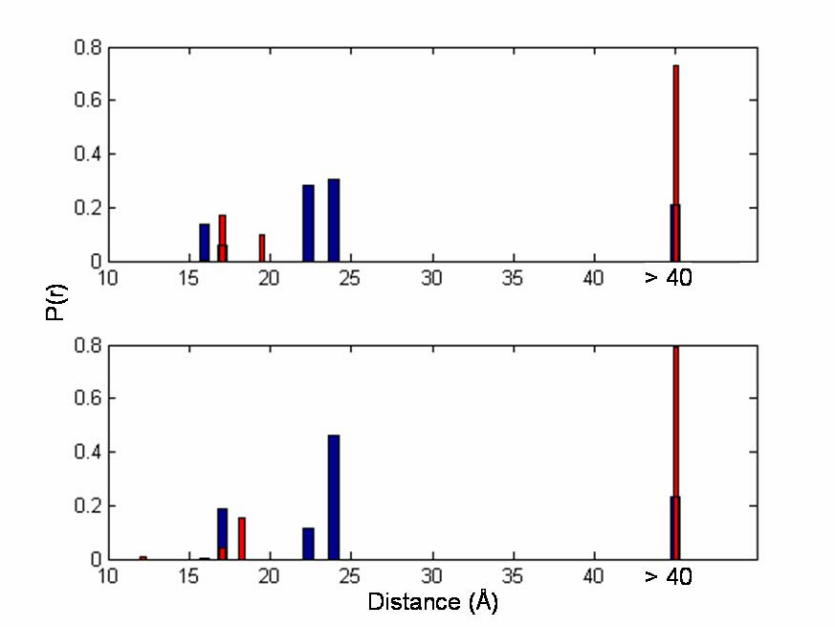

(a)

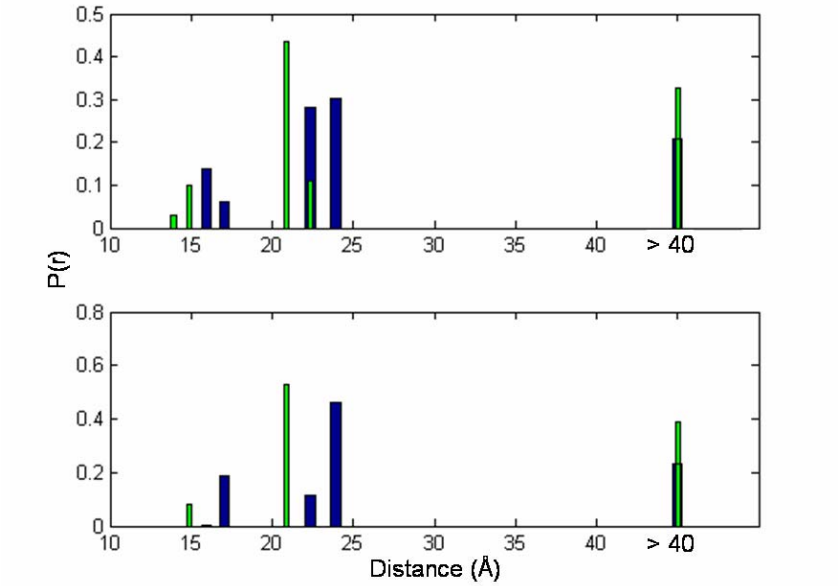

(b)

Figure 5.7. D-A distance distributions extrapolated from FET kinetics for W94/Y113(NO_2) (blue), **(a)** W94/Y113(NO_2)/A30P (red), and **(b)** W94/Y113(NO_2)/A53T (green) in 10 mM HEPES buffer (top panel), and 10 mM HEPES buffer with 1 mM Ca^{2+} (bottom panel)

The distance distributions between W94/Y125(NO_2) and W94/Y125(NO_2)/A30P are almost overlapping with each other, except that a higher population of extended distances (> 40 Å) is observed (**Figure 5.8a**). The lengthening caused by the addition of calcium ions observed in W94/Y125 is also demonstrated in W94/Y125(NO_2)/A30P. On the other hand, the presence of A53T mutants causes the mutant to shift to shorter distances when calcium ions are present (**Figure 5.8b**). Thus, an opposite trend is observed when calcium ions were added to A53T. This could suggest that while the presence of A30P and A53T mutants can cause more extended structures to form in solution, the A53T mutant can weaken the rigidity of the polypeptide 113–125, which was previously extrapolated in Chapter 4.

C-terminal Tail in SUVs.

In Chapter 4, it was suggested that there is a calcium binding region between residues 94 and 113, while a lengthening region can be found between residues 113 and 125. For W94/Y125(NO_2)/A30P (**Figure 5.9a**), there is an increase in the distance distribution, from 22 Å to 23 Å, when calcium ions are introduced. On the other hand, the distances extrapolated from the decay curves (not shown) for W94/Y125(NO_2)/A53T (**Figure 5.9b**), W94/Y113(NO_2)/A30P (**Figure 5.10a**), and W94/Y113(NO_2)/A53T (**Figure 5.10b**) when they are associated with SUVs show that all the distance populations can be found > 40 Å, demonstrating that there is negligible quenching, regardless of whether calcium ions were added. These distance distributions suggests that the lengthening region between 113 and 125 still persists when the single-point mutations were added. Therefore, calcium ions could still be

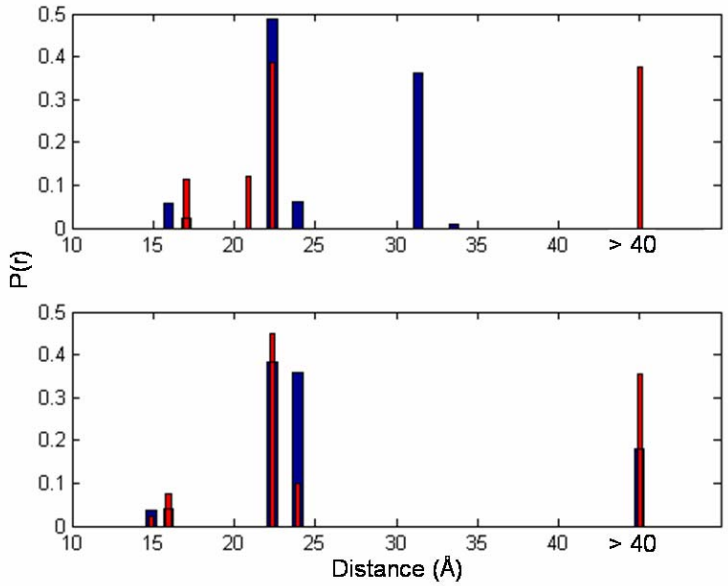

(a)

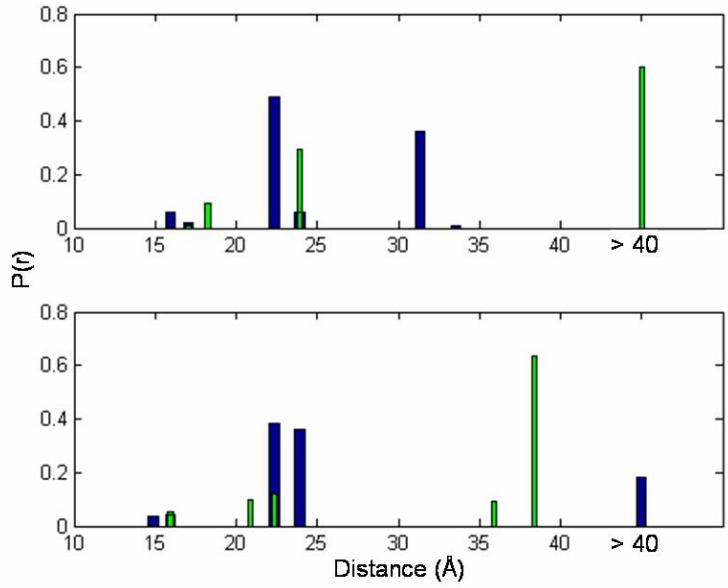

(b)

Figure 5.8. D-A distance distributions extrapolated from FET kinetics for W94/Y125(NO_2), **(a)** W94/Y125(NO_2)/A30P (red), and **(b)** W94/Y125(NO_2)/A53T (green) in 10 mM HEPES buffer (top panel), and 10 mM HEPES buffer with 1 mM Ca^{2+} (bottom panel)

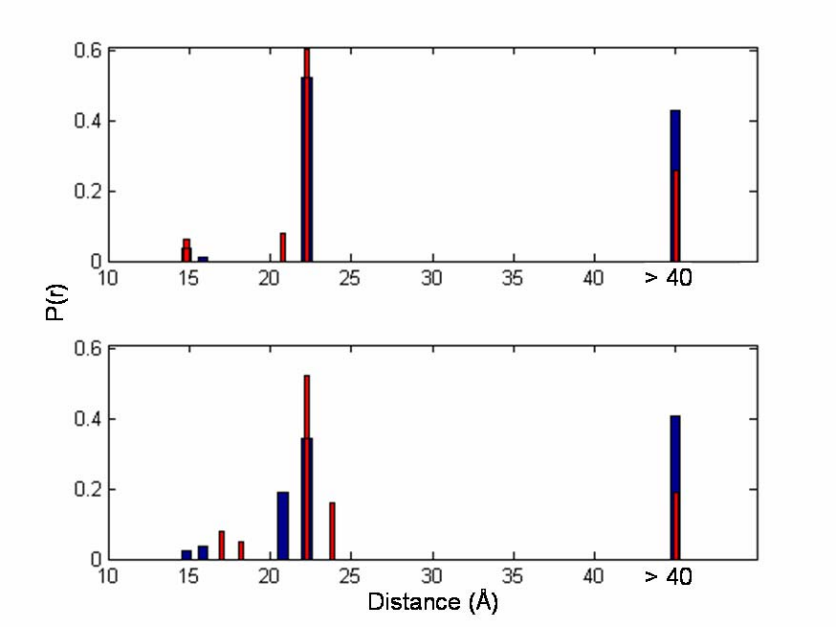

(a)

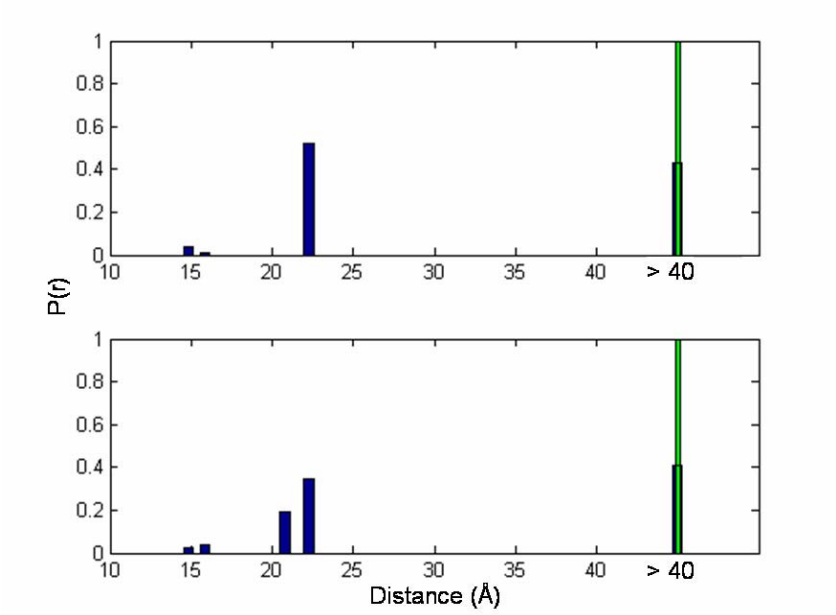

(b)

Figure 5.9. D-A distance distributions extrapolated from FET kinetics for W94/Y125(NO_2) (blue), **(a)** W94/Y125(NO_2)/A30P (red), and **(b)** W94/Y125(NO_2)/A53T (green) in 1:1 POPC:POPA (1.4 mg/mL)in 10 mM HEPES buffer (top panel), and with 1 mM Ca^{2+} (bottom panel)

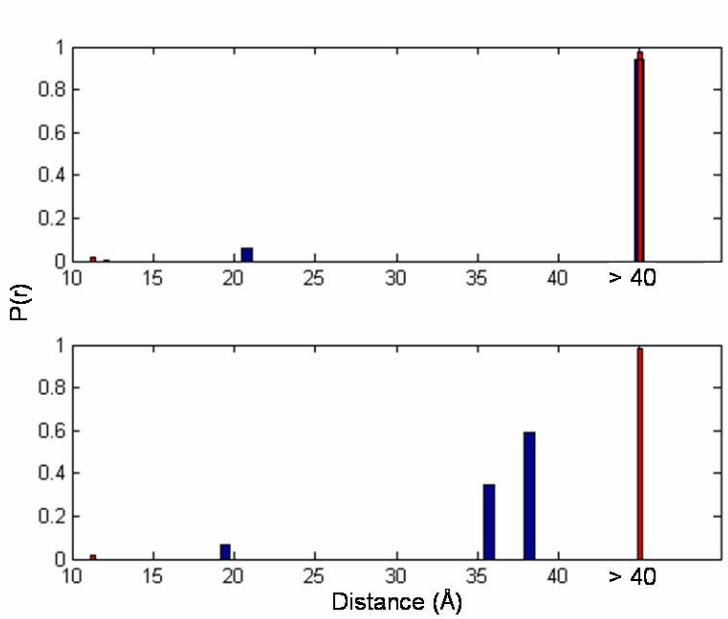

(a)

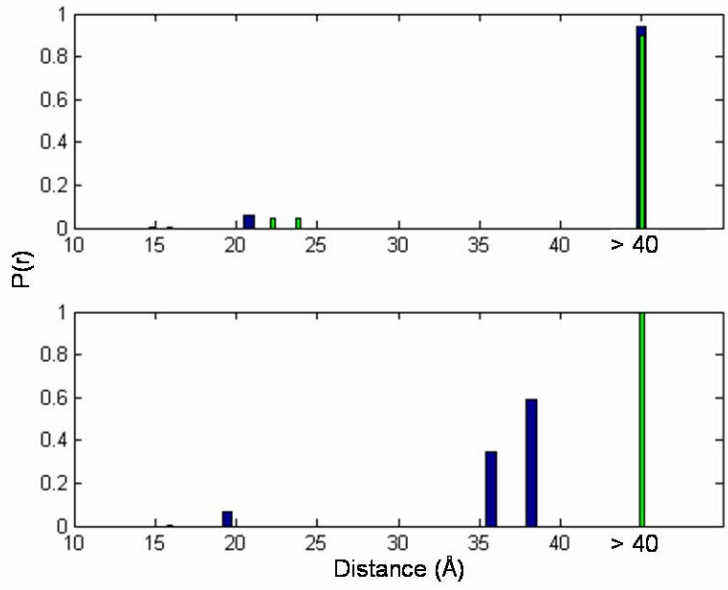

(b)

Figure 5.10. D-A distance distributions extrapolated from FET kinetics for W94/Y113(NO_2) (blue), **(a)** W94/Y113(NO_2)/A30P (red), and **(b)** W94/Y113(NO_2)/A53T (green) in 1:1 POPC:POPA (1.4 mg/mL)in 10 mM HEPES buffer (top panel), and with 1 mM Ca^{2+} (bottom panel)

affecting the C-terminal tail. However, the calcium binding region between 101 and 113 could be severely weakened with the introduction of the A30P or A53T mutations.

The distance distributions for W125/Y136(NO_2) in the presence of SUVs (**Figure 5.11**) suggest that there is a disappearance of calcium binding region between residues 125–136, as no intermediate or short distances emerge when calcium ions were added. However, a population (~ 60%) starts to appear when W125/ Y136(NO_2)/A30P (22 Å) and W125/Y136(NO_2)/A53T (21 Å) are associated with SUVs. What is more interesting is that upon the addition of calcium ions, a small degree of distance contraction can be observed.

Summary on the C-terminal Tail Region.

In conclusion, both the A30P and A53T mutations seem to generate more compact structures in solution and in SUVs, regardless of whether calcium ions were present. These single point mutations also affect the calcium binding ability of the first calcium binding region (polypeptide 101–113) when SUVs were present. On the contrary, the weak second calcium binding region (residues 125–136) seems to be enhanced slightly with these single-point mutations. In solution, the first calcium binding region seems to be maintained, while the second binding region is enhanced.

Since more compact structures are formed with the mutations, these structures could encourage the formation of protofibrils. The two calcium binding regions could serve a different role in the pathogenesis of the disease, as one of them is enhanced in the presence of SUVs, while the other one is weakened. However, the

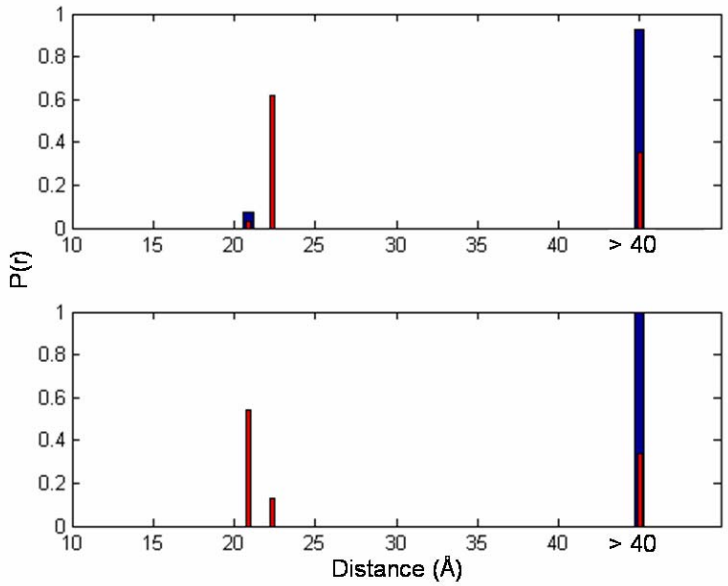

(a)

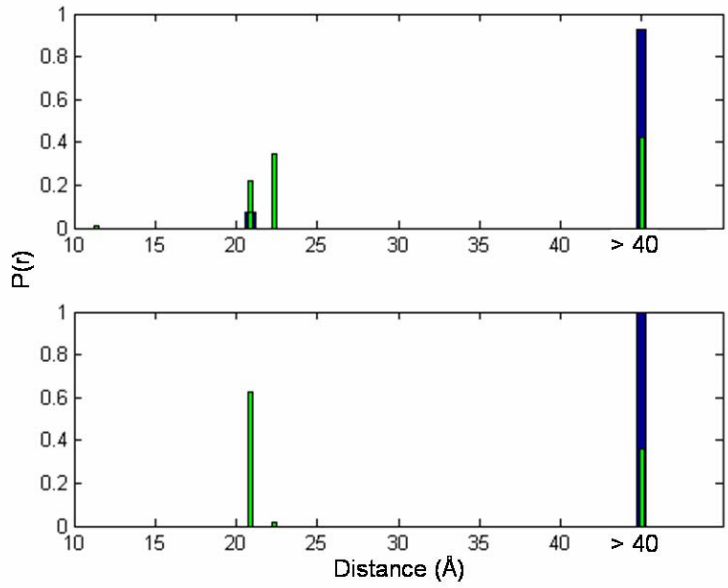

(b)

Figure 5.11. D-A distance distributions extrapolated from FET kinetics for W125/Y136(NO_2) (blue), **(a)** W125/Y136(NO_2)/A30P (red), and **(b)** W125/Y136(NO_2)/A53T (green) in 1:1 POPC:POPA (1.4 mg/mL)in 10 mM HEPES buffer (top panel), and with 1 mM Ca^{2+} (bottom panel)

change in the calcium binding ability of this C-terminal tail caused by these mutations can show that calcium ions are also quite important in determining the monomeric structure of α-syn, possibly influencing the rate of plaque formation.

5.5 ACKNOWLEDGEMENTS

This project was completed with the assistance of Ms. Stephanie S. E. Schulze, Mr. Matthew L. Robinson, and Ms. Debbie G. Tseng.

5.6 REFERENCES

(1) Kruger, R.; Kuhn, W.; Muller, T.; Woitalla, D.; Graeber, M.; Kosel, S.; Przuntek, H.; Epplen, J. T.; Schols, L.; Riess, O. *Nat. Genet.* **1998**, *18*, 106–108.

(2) Polymeropoulos, M. H.; Lavedan, C.; Leroy, E.; Ide, S. E.; Dehejia, A.; Dutra, A.; Pike, B.; Root, H.; Rubenstein, J.; Boyer, R.; Stenroos, E. S.; Chandrasekharappa, S.; Athanassiadou, A.; Papapetropoulos, T.; Johnson, W. G.; Lazzarini, A. M.; Duvoisin, R. C.; Di Iorio, G.; Golbe, L. I.; Nussbaum, R. L. *Science* **1997**, *276*, 2045–2047.

(3) Rochet, J. C.; Outeiro, T. F.; Conway, K. A.; Ding, T. T.; Volles, M. J.; Lashuel, H. A.; Bieganski, R. M.; Lindquist, S. L.; Lansbury, P. T. *J. Mol. Neurosci.* **2004**, *23*, 23–33.

(4) Narhi, L.; Wood, S. J.; Steavenson, S.; Jiang, Y. J.; Wu, G. M.; Anafi, D.; Kaufman, S. A.; Martin, F.; Sitney, K.; Denis, P.; Louis, J. C.; Wypych, J.; Biere, A. L.; Citron, M. *J. Biol. Chem.* **1999**, *274*, 9843–9846.

(5) Conway, K. A.; Harper, J. D.; Lansbury, P. T. *Nat. Med.* **1998**, *4*, 1318–1320.

(6) El-Agnaf, O. M. A.; Jakes, R.; Curran, M. D.; Wallace, A. *Febs Letters* **1998**, *440*, 67–70.

(7) Hashimoto, M.; Hsu, L. J.; Sisk, A.; Xia, Y.; Takeda, A.; Sundsmo, M.; Masliah, E. *Brain Res.* **1998**, *799*, 301–306.

(8) Giasson, B. I.; Uryu, K.; Trojanowski, J. Q.; Lee, V. M. Y. *J. Biol. Chem.* **1999**, *274*, 7619–7622.

(9) Conway, K. A.; Harper, J. D.; Lansbury, P. T. *Biochemistry* **2000**, *39*, 2552–2563.

(10) Li, J.; Uversky, V. N.; Fink, A. L. *Biochemistry* **2001**, *40*, 11604–11613.

(11) Li, J.; Uversky, V. N.; Fink, A. L. *Neurotoxicology* **2002**, *23*, 553–567.

(12) Jo, E. J.; McLaurin, J.; Yip, C. M.; St George-Hyslop, P.; Fraser, P. E. *J. Biol. Chem.* **2000**, *275*, 34328–34334.

(13) McLean, P. J.; Kawamata, H.; Ribich, S.; Hyman, B. T. *J. Biol. Chem.* **2000**, *275*, 8812–8816.
(14) Perrin, R. J.; Woods, W. S.; Clayton, D. F.; George, J. M. *J. Biol. Chem.* **2000**, *275*, 34393–34398.
(15) Jensen, P. H.; Nielsen, M. S.; Jakes, R.; Dotti, G.; Goedert, M. *J. Biol. Chem.* **1998**, *273*, 26292–26294.
(16) Ding, T. T.; Lee, S. J.; Rochet, J. C.; Lansbury, P. T. *Biochemistry* **2002**, *41*, 10209–10217.
(17) Bussell, R.; Eliezer, D. *J. Mol. Biol.* **2003**, *329*, 763–778.
(18) Chandra, S.; Chen, X. C.; Rizo, J.; Jahn, R.; Sudhof, T. C. *J. Biol. Chem.* **2003**, *278*, 15313–15318.
(19) Eliezer, D.; Kutluay, E.; Bussell, R.; Browne, G. *J. Mol. Biol.* **2001**, *307*, 1061–1073.
(20) Jao, C. C.; Der-Sarkissian, A.; Chen, J.; Langen, R. *Proc. Natl. Acad. Sci. U. S. A.* **2004**, *101*, 8331–8336.
(21) Ramakrishnan, M.; Jensen, P. H.; Marsh, D. *Biochemistry* **2003**, *42*, 12919–12926.
(22) Ulmer, T. S.; Bax, A.; Cole, N. B.; Nussbaum, R. L. *J. Biol. Chem.* **2005**, *280*, 9595–9603.
(23) George, J. M.; Jin, H.; Woods, W. S.; Clayton, D. F. *Neuron* **1995**, *15*, 361–372.
(24) Lee, J. C.; Langen, R.; Hummel, P. A.; Gray, H. B.; Winkler, J. R. *Proc. Natl. Acad. Sci. U. S. A.* **2004**, *101*, 16466–16471.